Electronic Supplementary Information for

An all-inorganic quasi-homogenous polyoxometalate/$[Mo_3S_{13}]^{2-}$ system for efficient and stable photocatalytic H_2 evolution

Wenbo Li,[a,b,c] Shixiong Min,*[a,b,c] Fang Wang[a,b,c] and Zhengguo Zhang[a,b,c]

[a] *School of Chemistry and Chemical Engineering, Key Laboratory of Electrochemical Energy Conversion Technology and Application, North Minzu University, Yinchuan, 750021, P. R. China. E-mail: sxmin@nun.edu.cn.*

[b] *Key Laboratory of Chemical Engineering and Technology, State Ethnic Affairs Commission, North Minzu University, Yinchuan, 750021, P. R. China.*

[c] *Ningxia Key Laboratory of Solar Chemical Conversion Technology, North Minzu University, Yinchuan 750021, P. R. China.*

1. Experimental section

1.1 Chemicals and materials

All chemicals were of analytical grade and used as received without further purification. $H_4SiW_{12}O_{40}$ (SiW_{12}) powders were purchased from Tianjin Guangfu Fine Chemical Research Institute. $(NH_4)_6Mo_7O_{24}\cdot 4H_2O$ and $(NH_4)_2S$ solution were received from Shanghai Aladdin Biochemical Technology Co. Ltd. All solutions used throughout the experiments were prepared with ultrapure water (18.2 MΩ).

1.2 Characterization

X-ray diffraction (XRD) patterns were investigated with a Rigaku smartlab diffractometer with a nickel filtrated Cu Kα radiation. X-ray photoelectron spectroscopy (XPS) measurements of the samples were performed on an X-ray photoelectron spectrometer (Thermo Scientific Escalab-250Xi) equipped with a monochromatic Al Ka X-ray source. Binding energies were referenced to the C 1s peak (set at 284.8 eV) of the sp^2 hybridized (C=C) carbon from the sample. Ultraviolet-visible (UV-vis) transmission spectroscopy was performed using a Shimadzu UV-1800 spectrophotometer. Photoluminescence spectra were determined by a Horiba Scientific FluoroMax-4 spectrofluorometer spectrometer.

1.3 Preparation of catalysts

1.3.1 $[Mo_3S_{13}]^{2-}$ nanoclusters

The thiomolybdate $(NH_4)_2Mo_3S_{13}\cdot xH_2O$ (x=0~2) was prepared by a the method developed by Müller *et al.*[1] Briefly, 4.0 g of $(NH_4)_6Mo_7O_{24}\cdot 4H_2O$ was dissolved in 20 mL of water in an Erlenmeyer flask. An ammonium polysulfide solution (120 ml, 25 wt%)

was added and the flask was covered with a watch glass. The solution was then kept on an oil bath (96℃) for five days without stirring. Dark-red crystals of $(NH_4)_2Mo_3S_{13}\cdot xH_2O$ precipitated and were removed by filtering, followed by washing successively with water and ethanol. To remove excess sulfur, the $(NH_4)_2Mo_3S_{13}\cdot xH_2O$ crystals were first heated in hot toluene (80 ℃) for 2~4 h followed washed by dimethyl sulfoxide (DMSO) for several times. Finally, the crystals were dried in air and stored in darkness. Its XRD pattern is given in Fig. S1.

1.3.2 Preparation of well-crystallized MoS_2 nanoparticles

In a typical synthesis, 1.5 g of $(NH_4)_6Mo_7O_{24}$ was added to 20 ml of $(NH_4)_2S$ solution under stirring conditions. The mixture was then heated at 80 °C to obtain a deep red solution. The solution was stirred for 2 h and then transferred to a refrigerator with duration of 12 h. The precipitated red crystals were thoroughly washed with ethanol, dried, and stored under nitrogen. The MoS_2 nanoparticles were synthesized by thermal decomposition of $(NH_4)_2MoS_4$ in an N_2 atmosphere at 800 °C for 5 h with a ramping rate of 5 °C mim^{-1}. Its XRD pattern is given in Fig. S9.

1.3.3 Preparation of amorphous MoS_x

The a-MoS_x was synthesized by in situ photoreduction of $(NH_4)_2MoS_4$ (5 μmol) in a EtOH/H_2O (1/1, pH 2.4) solution containing SiW_{12} (0.5 mM) under the irradiation of a 300-W Xe lamp (CEL-HXF300) for 5 h.

1.4 Photocatalytic activity measurements

The photocatalytic hydrogen production experiments were performed in a sealed Pyrex reactor (250 mL) with a top flat quartz window for light irradiation and a silicone rubber

septum was fixed on its side for sampling produced H_2 in the headspace of reaction cell. A 300 W Xe lamp (CEL-HXF300) equipped no cut-off filter was used as light source. In a typical experiment, SiW_{12} and the $[Mo_3S_{13}]^{2-}$ catalyst were added to 100 mL EtOH/H_2O (1/1, pH 2.4) solution, with magnetic stirring. Then, the reaction solution was thoroughly degassed by repeated evacuation-N_2 filling, and finally refilled with N_2 to reach ambient pressure. After that, the reaction solution was irradiated under continuous stirring. The amount of H_2 produced was manually taken out by a gas-tight syringe (Agilent, 1.0 mL) and analyzed at given time intervals with a precalibrated gas chromatography (Tech comp; GC-7900) with a thermal conductivity detector, a 5 Å molecular sieve column (4 mm×5 m), and with N_2 as carrying gas. Before irradiation, the reaction system was thoroughly degassed by evacuation. solution was maintained at 6 °C by a flow of cooling water during the photocatalytic reaction.

1.5 Electrochemical measurements

The electrochemical measurements were carried out in a standard three-electrode electrochemical set-up using a CS3103 (Wuhan Corrtest Instruments Corp., Ltd) electrochemical workstation. A platinum (Pt) mesh (1 cm×1 cm) and a saturated calomel electrode (SCE) were used as the counter electrode and reference electrode, respectively. Glassy carbon (GC, diameter: 3 mm) was used as the working electrode. The GC electrode was polished with alumina powders and subsequently cleaned with deionized water, ethanol and acetone each for 10 min by ultrasonication to obtain a mirror surface. A 0.1 M Na_2SO_4 (pH 2.4) solution was used as the supporting electrolyte. N_2 gas was bubbled continuously for remove oxygen during the testing. Potential were converted to NHE potentials by using E(NHE)=E(SCE)+0.240 V. Bulk electroreduction of SiW_{12} at a

constant applied potential was performed in a 0.1 M Na_2SO_4 (pH 2.4) solution using a carbon paper (1.5 cm×1.5 cm) as the working electrode.

2. Additional figures and table

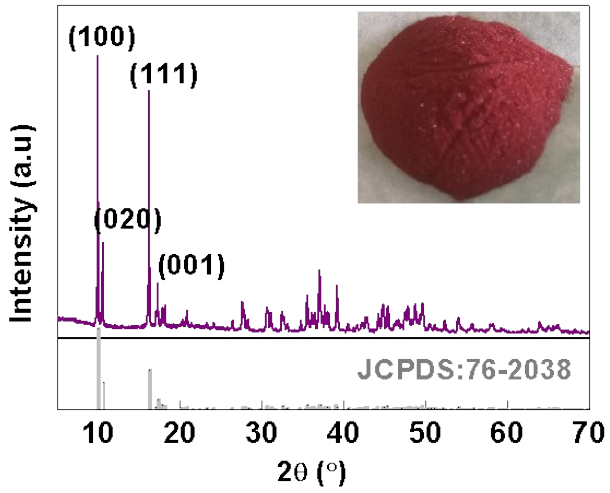

Fig. S1 XRD pattern of $(NH_4)_2Mo_3S_{13}$. Inset shows the digital photos of $(NH_4)_2Mo_3S_{13}$ powders

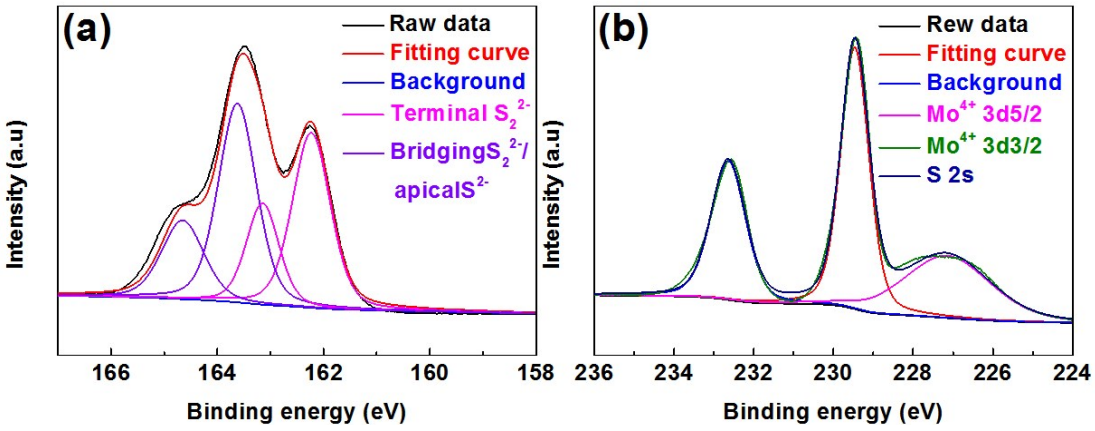

Fig. S2 High resolution (a) S 2p and (b) Mo 3d XPS spectra of $(NH_4)_2Mo_3S_{13}$.

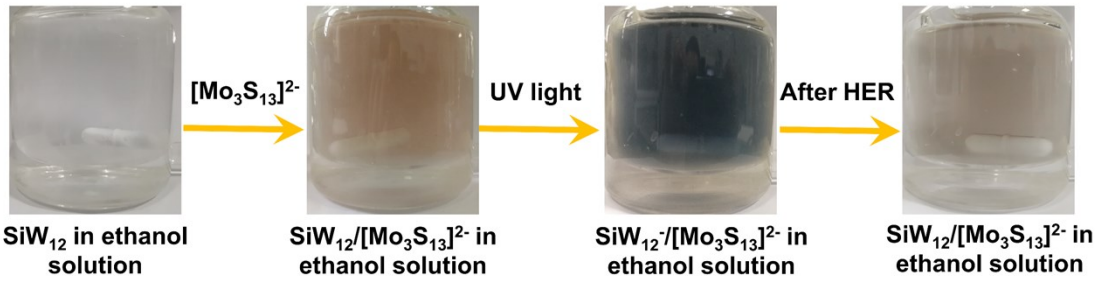

Fig. S3 Schematic diagram of the $SiW_{12}/[Mo_3S_{13}]^{2-}$ HER process.

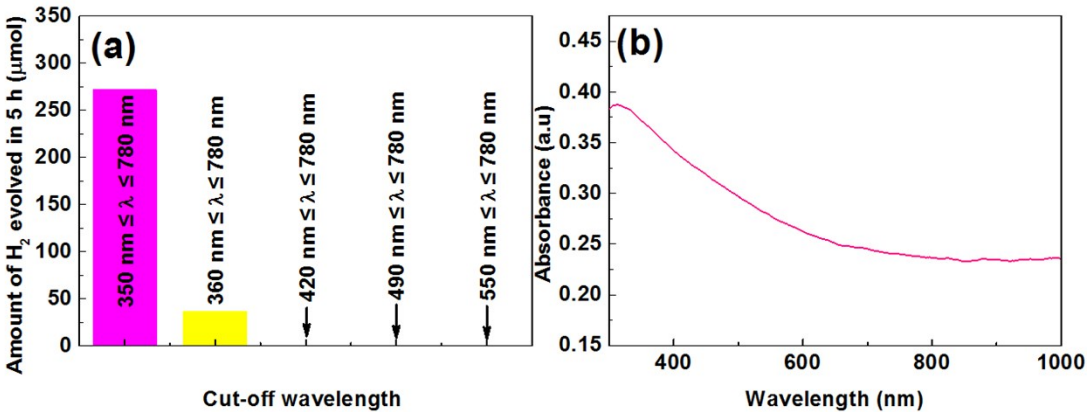

Fig. S4 (a) H_2 evolution from $SiW_{12}/[Mo_3S_{13}]^{2-}$ system in $EtOH/H_2O$ (1/1) solution (pH 2.4) under the light irradiation of different cut-off wavelengths. Reaction conditions: SiW_{12}, 0.5 mM; $[Mo_3S_{13}]^{2-}$, 50 μM; light source, 300-W Xe lamp (350 nm≤λ≤780 nm). (b) UV-vis spectrum of $[Mo_3S_{13}]^{2-}$ in $EtOH/H_2O$ (1/1) solution (pH 2.4).

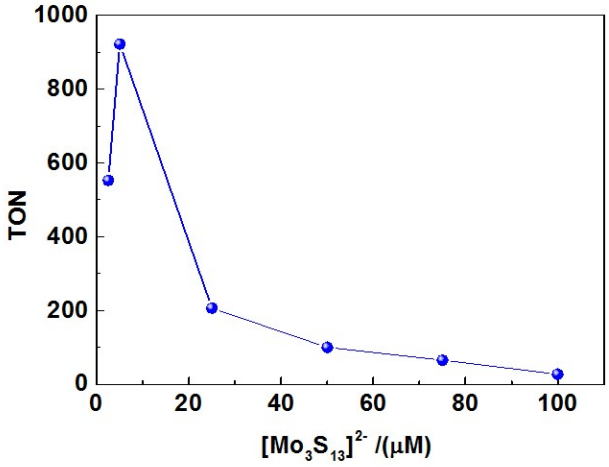

Fig. S5 TON of H_2 evolution from $SiW_{12}/[Mo_3S_{13}]^{2-}$ system in $EtOH/H_2O$ (1/1, 100 mL, pH 2.4) solution. Reaction conditions: SiW_{12}, 0.5 mM; light source, 300-W Xe lamp (350 nm ≤λ≤780 nm).

Table S1 Comparison of H_2 evolution activity of $SiW_{12}/[Mo_2S_{13}]^{2-}$ system with other systems/photocatalysts using molecular Mo-S based catalysts.

Catalyst	Photosensitizer	Reaction conditions	Light source	TON	Ref.
$[Mo_3S_{13}]^{2-}$	pom-CN	LA (10 vol.%), 100 mL	300-W Xe lamp, ≥420 nm	22 (1 h)	2
$[Mo_3S_{13}]^{2-}$	$Ru(bpy)_3Cl_2$	CH_3CN/H_2O (100 mL, 9/1), H_2A(100 mM)	300 W Xe lamp, ≥420 nm	1570 (5 h)	3
$[Mo_3S_{13}]^{2-}$	CdTe/CdS	H_2A (20 mg/mL), 20 mL	300-W Xe lamp, ≥420 nm	12778 (20 h)	4
$[Mo_2S_{12}]^{2-}$	$Ru(bpy)_3Cl_2$	$MeOH/H_2O$ (10/1), H_2A (100 mM)	LED light, ≥470 nm	1750 (12 h)	5
$[Mo_2S_{12}]^{2-}$	Fluorescein	$MeOH/H_2O$ (1/1), TEA (10 vol%)	300-W Xe lamp, ≥420 nm	33 (1 h)	6
$[Mo_2S_{13}]^{2-}$@EB-COF	$Ru(bpy)_3Cl_2$	DMF/H_2O (1/1), H_2A (300 mM)		51 (1 h)	
$[Mo_2S_{13}]^{2-}$	SiW_{12}	EtOH/H_2O (1/1), pH 2.4	300-W Xe lamp 350 nm ≤λ≤780 nm	6879 (40 h)	This work

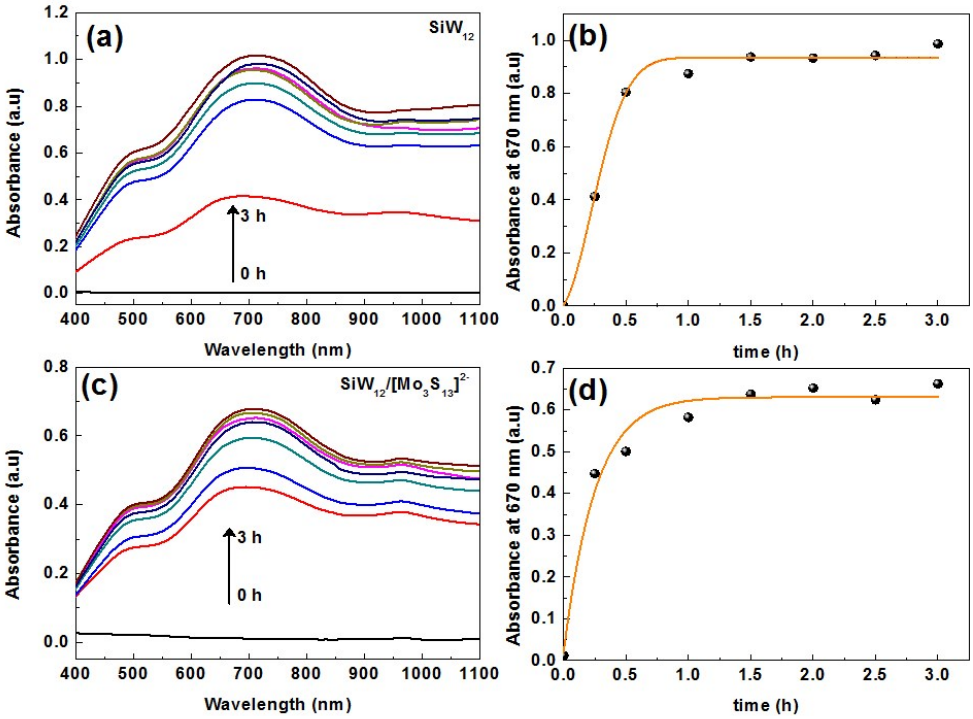

Fig. S6 UV-vis absorption spectra of the system containing SiW_{12} (0.5 mM) in EtOH/H_2O (1/1, pH 2.4) upon light irradiation (300 W Xe lamp, 350 nm≤λ≤780 nm) (a) without $[Mo_3S_{13}]^{2-}$ and (c) with $[Mo_3S_{13}]^{2-}$ (5 mM), and the corresponding changes in absorbance at 670 nm are shown in panels (b) and (d), respectively.

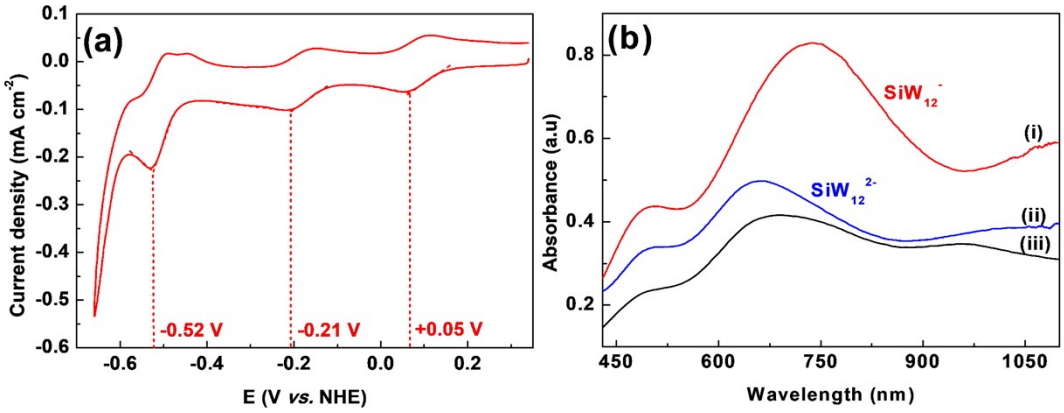

Fig. S7 (a) CV curve of SiW_{12} (0.5 mM) recorded in a 0.1 M Na_2SO_4 solution (pH 2.4) with a scan rate of 50 mV s^{-1}. (b) UV-vis absorption spectra of electrochemically reduced SiW_{12} (0.5 mM) at (i) -0.08 V and (ii) -0.37 V vs. NHE for 1 h in a 0.1 M Na_2SO_4 solution (pH 2.4) along with the (iii) UV-vis absorption spectrum of system containing SiW_{12} (0.5 mM) in EtOH/H_2O (1/1, pH 2.4) after 3 h of light irradiation (300-W Xe lamp, 350 nm≤λ≤780 nm) for a comparison.

It has been reported that Keggin-type SiW_{12} typically undergoes two successive one-electron reduction to form two-electron reduced product, eventually form multielectron-reduced products by accepting more electrons in the common pH domains.[7,8] Accordingly, in a typical CV curve of SiW_{12}, several reduction waves could be observed in the approximate electron ratios 1:1:2:8:12.[7] In Fig. S7a, the whole CV curve for a 0.5 mM SiW_{12} solution at pH 2.4 also consists of three main redox waves located at +0.05 V, -0.21 V, and -0.52 V vs. NHE, and the separations between cathodic and anodic peak potentials for each redox wave are 55 mV, 55 mV, and 30 mV, respectively. These values fit the 1: 1: 2 electron ratios. Therefore, the reversible redox wave observed at -0.21 V vs. NHE in Fig. S7a can be attributable to the second one-electron reduction of SiW_{12} to produce two-electron reduction product SiW_{12}^{2-} rather than one-electron reduction product SiW_{12}^{-}. In order to further confirm this conclusion, as shown in Fig. S7b, we have also collected the UV-vis absorption spectra of SiW_{12} electrochemically reduced at one-electron (-0.08 V vs. NHE) and two-electron (-0.37 V vs. NHE) reduction potentials and compared them with the UV-vis absorption spectrum of SiW_{12} after UV light irradiation. It can be clearly seen that the UV-vis absorption spectra of both the SiW_{12}^{-} and SiW_{12}^{2-} are well consistent with those of reported ones in the literature[9], and the UV-

vis absorption spectrum of SiW_{12} after UV light irradiation is similar to that of SiW_{12}^{2-}. As also can be seen from Fig. 2c that, an obvious reduction event corresponding to H_2 evolution occurs at essentially the same potential as the second reduction of SiW_{12} in the presence of $[Mo_3S_{13}]^{2-}$, which suggests that the electron transfer from SiW_{12}^{2-} to $[Mo_3S_{13}]^{2-}$ is a thermodynamically feasible process. These results firmly confirms that the SiW_{12}^{2-} rather than SiW_{12}^{-} is the key reaction intermediate that can transfer electrons to the $[Mo_3S_{13}]^{2-}$ clusters to induce an efficient H_2 evolution reaction.

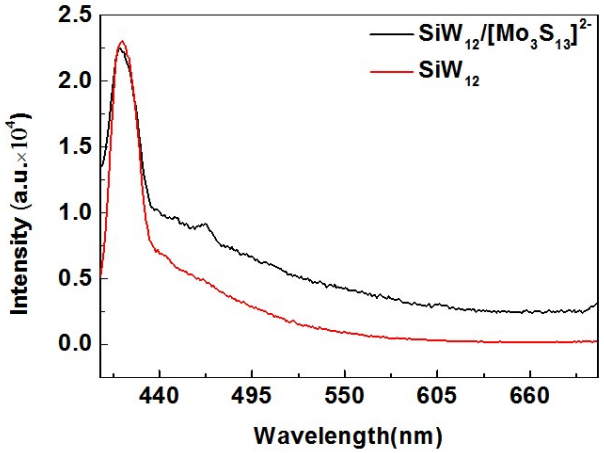

Fig. S8 Steady-state PL spectra of SiW_{12} upon light irradiation in EtOH/H_2O (1/1, pH 2.4) with and without $[Mo_3S_{13}]^{2-}$. The excitation wavelength is 370 nm.

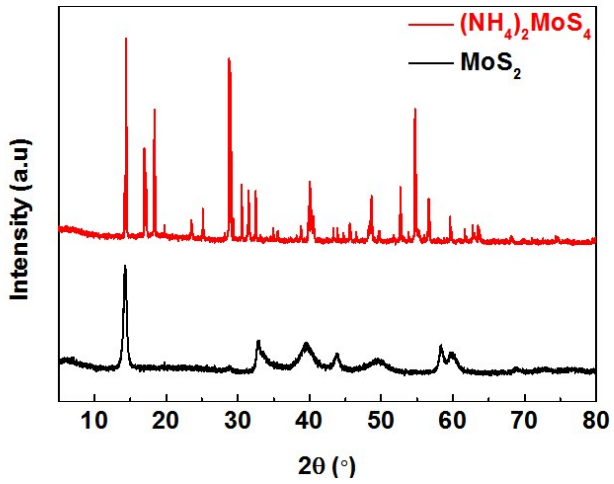

Fig. S9 XRD patterns of $(NH_4)_2MoS_4$ and MoS_2.

References

1. A. Müller, E. Krickemeyer, A. Hadjikyriacou and D. Coucouvanis, *Inorganic Syntheses*, 2007, **27**, 47.

2. F. S. Guo, Y. D. Hou, A. M. Asiri and X. C. Wang, *Chem. Commun.*, 2017, **53**, 13221.

3. Y. G. Lei, M. Q. Yang, J. H. Hou, F. Wang, E. T. Cui, C. Kong and S. X. Min, *Chem. Commun.,* 2018, **54**, 603.

4. D. T. Yue, X. F. Qian, Z. C. Zhang, M. Kan, M. Ren and Y. X. Zhao, *ACS Sustainable Chem. Eng.,* 2016, **12**, 6653.

5. A. Rajagopal, F. Venter, T. Jacob, L. Petermann, S. Rau, S. Tschierlei and C. Streb, *Sustain. Energy Fuels,* 2019, **3**, 92.

6. Y. J. Cheng, R. Wang, S. Wang, X. J. Xi, L. F. Ma and S. Q. Zang, *Chem. Commun.,* 2018, **54**, 13563.

7. B. Keita and L. Nadjo, *J. Electroanal. Chem*., 1987, **217**, 287.

8. J. Lei, J. J. Yang, T. Liu, D. R. Deng, M. S. Zheng, J. J. Chen, L. Cronin and Q. F. Dong, *Chem. Eur. J.,* 2019, **25**, 11432.

9. B. Rausch, M. Symes, G. Chisholm, and L. Cronin, *Science,* 2014, **345**, 1326.